

# Attention Isn't All You Need for Emotion Recognition: Domain Features Outperform Transformers on the EAV Dataset

Anmol Guragain

Universidad Politécnica de Madrid  
E.T.S. Ingenieros de Telecomunicación  
anmol.g@upm.es

## Abstract

We present a systematic study of multimodal emotion recognition using the EAV dataset, investigating whether complex attention mechanisms improve performance on small datasets. We implement three model categories: baseline transformers (M1), novel factorized attention mechanisms (M2), and improved CNN baselines (M3). Our experiments show that sophisticated attention mechanisms consistently underperform on small datasets. M2 models achieved 5 to 13 percentage points below baselines due to overfitting and destruction of pretrained features. In contrast, simple domain-appropriate modifications proved effective: adding delta MFCCs to the audio CNN improved accuracy from 61.9% to **65.56%** (+3.66pp), while frequency-domain features for EEG achieved **67.62%** (+7.62pp over the paper baseline). Our vision transformer baseline (M1) reached **75.30%**, exceeding the paper's ViViT result (74.5%) through domain-specific pretraining, and vision delta features achieved **72.68%** (+1.28pp over the paper CNN). These findings demonstrate that for small-scale emotion recognition, domain knowledge and proper implementation outperform architectural complexity.

## 1 Introduction

Emotion recognition from physiological and behavioral signals is a core challenge in affective computing, with applications in human-computer interaction, mental health monitoring, and assistive technologies. The EAV dataset (Kim et al., 2024) provides synchronized EEG, Audio, and Video recordings from 42 participants engaged in conversational interactions, offering a unique resource for multimodal emotion research. However, with only approximately 280 training samples per subject after data splitting, this dataset presents significant challenges for deep learning approaches.

This limited data availability motivates our central research question: *Do complex attention mech-*

*anisms improve emotion recognition performance on small datasets, or do simpler approaches with domain-appropriate features perform better?*

To answer this question, we systematically evaluate three categories of models. First, we implement baseline transformer architectures (M1) to establish reference performance. Second, we develop novel factorized attention mechanisms (M2) tailored to each modality's unique structure: spatial-temporal-asymmetry attention for EEG, temporal-frequency dual attention for audio, and ViViT-style space-time attention for video. Third, we explore minimal CNN improvements (M3) focusing on bug fixes and domain-appropriate feature engineering.

Our study makes three contributions: (1) we show that factorized attention mechanisms consistently fail on small datasets, underperforming baselines by 5 to 13 percentage points; (2) we demonstrate that simple, domain-appropriate modifications (delta MFCCs for audio and band power features for EEG) achieve state-of-the-art results on this dataset; and (3) we provide analysis of failure modes and success factors for emotion recognition on limited data.

## 2 Related Work

### 2.1 Emotion Recognition Datasets

Traditional EEG datasets such as DEAP (Koelstra et al., 2012) and MAHNOB-HCI employ passive elicitation paradigms where participants watch emotional stimuli. Audio-visual datasets like IEMOCAP (Busso et al., 2008) capture conversational emotions but lack neurophysiological signals. The EAV dataset bridges this gap by providing synchronized multimodal recordings during active conversation, though its relatively small scale (42 participants) constrains the complexity of applicable models.

## 2.2 Transformer Architectures for Emotion Recognition

The Audio Spectrogram Transformer (AST) (Gong et al., 2021) treats spectrograms as images, applying Vision Transformer architecture with strong performance on large-scale audio datasets. Video Vision Transformer (ViViT) (Arnab et al., 2021) extends this approach to video through factorized space-time attention, achieving  $22\times$  computational efficiency over full attention. EEGformer (Husain and Park, 2022) adapts transformers for EEG signals. These architectures achieve impressive results on large datasets, but their effectiveness on small-scale emotion recognition remains unclear.

## 2.3 Frontal Asymmetry in Emotion

Davidson’s frontal asymmetry model (Davidson, 1992) establishes that left frontal cortex activation (measured at F3) correlates with approach motivation and positive emotions, while right frontal activation (F4) correlates with withdrawal motivation and negative emotions. This neurophysiological insight motivates our M2 EEG architecture and M3 band power features.

## 2.4 Feature Engineering for Emotion Recognition

Classical approaches to emotion recognition rely on hand-crafted features. For EEG, band power and differential entropy features computed from frequency bands (delta, theta, alpha, beta, gamma) have proven effective on the SEED dataset (Zheng and Lu, 2015). For audio, Mel-frequency cepstral coefficients (MFCCs) and their temporal derivatives (delta and delta-delta) capture both spectral content and dynamics (Schuller et al., 2013). Squeeze-and-Excitation networks (Hu et al., 2018) introduced channel attention for CNNs, learning to weight feature map importance through a bottleneck architecture.

## 3 Dataset

The EAV dataset contains recordings from 42 participants, each providing 200 interaction samples across five emotion classes: Neutral, Anger, Happiness, Sadness, and Calmness. EEG signals are recorded using a 30-channel BrainAmp system at 500 Hz, audio at 16 kHz, and video at 30 fps.

Following standard preprocessing, EEG signals are downsampled to 100 Hz and bandpass filtered (0.5 to 45 Hz), yielding segments of shape (30

channels, 500 samples). Audio clips of 5 seconds are extracted, and 25 video frames are sampled per segment. The data is split 70/30 for training and testing per subject, resulting in approximately 280 training and 120 test samples per subject per modality.

This limited training data (280 samples with 15,000 EEG features, 80,000 audio samples, or  $25\times 224\times 224\times 3$  video pixels) fundamentally constrains model complexity and motivates our investigation of simpler approaches.

## 4 Methods

### 4.1 M1: Baseline Transformer Architectures

Our baseline models replicate the paper’s transformer approach using pretrained architectures from Hugging Face.

**EEG Transformer.** We implement a custom architecture with convolutional feature extraction followed by transformer encoding. Two 1D convolutional layers (kernel size 11, padding 5) transform the 30-channel input into 60-dimensional features while preserving temporal resolution. Six transformer encoder layers with 4 attention heads and hidden dimension 60 model temporal dependencies. Mean pooling followed by a two-layer classifier produces emotion predictions. This architecture applies standard self-attention across time, treating channels as input features rather than a separate dimension.

**Audio Spectrogram Transformer.** We fine-tune the pretrained AST model (MIT/ast-finetuned-audioset) with a custom 5-class classifier head. The model converts audio waveforms to mel spectrograms ( $1024\times 128$ ), extracts  $16\times 16$  patches yielding approximately 1212 tokens, and applies 12 transformer layers with 768-dimensional embeddings. Training proceeds in two stages: 10 epochs with frozen backbone (learning rate 5e-4), followed by 15 epochs with unfrozen backbone (learning rate 5e-6).

**Vision Transformer.** We employ a ViT model pretrained on facial emotion recognition (dima806/facial\_emotions\_image\_detection). Each video is processed as 25 independent frames, with per-frame predictions averaged for the final classification. The same two-stage training strategy is applied: 10 epochs frozen, then 5 epochs

unfrozen. While this approach ignores temporal dynamics across frames, the facial emotion pretraining provides strong baseline performance.

## 4.2 M2: Factorized Attention Mechanisms

Our main architectural contribution explores whether factorized attention, tailored to each modality’s structure, can improve upon baselines. Figure 1 illustrates the three M2 architectures.

### 4.2.1 M2-EEG: Tri-Stream Transformer

EEG signals contain information along three distinct axes. The spatial dimension captures relationships between brain regions (channels), the temporal dimension captures signal dynamics, and the hemispheric asymmetry dimension captures left-right differences relevant for emotional valence.

Our architecture first applies convolutional feature extraction, then branches into three parallel attention streams. The spatial stream transposes features to (time, channels, features) and applies attention across channels, learning which brain regions interact at each time point. The temporal stream applies attention across time points for each channel, capturing event-related dynamics. The asymmetry stream computes difference signals between six hemisphere pairs (Fp1-Fp2, F3-F4, F7-F8, C3-C4, P3-P4, O1-O2) based on the 10-20 electrode system, then applies attention across these pairs. Following Davidson’s model, F3-F4 receives a  $1.2 \times$  attention weight.

Stream outputs are fused using learned softmax weights, with a learnable skip connection preserving convolutional features. The skip weight is initialized such that approximately 73% of the signal comes from the convolutional path. We explored three model sizes (138K, 419K, and 1.6M parameters), with the smallest recommended for this dataset size.

### 4.2.2 M2-EEG: EEGNet-Improved

As a literature-based alternative, we enhanced EEGNet with techniques from recent papers: squeeze-excitation blocks for channel attention, multi-scale temporal convolution (kernels 16, 32, 64), residual connections, data augmentation (amplitude scaling, Gaussian noise, time shift), label smoothing (0.1), AdamW optimizer with weight decay, and cosine annealing learning rate schedule.

### 4.2.3 M2-Audio: Temporal-Frequency Dual Attention

Audio spectrograms have natural 2D structure: the temporal axis captures speech rhythm, pauses, and intensity changes, while the frequency axis captures pitch, harmonics, and voice quality. Standard AST flattens this structure into a 1D patch sequence, losing the distinction.

Our architecture preserves AST’s pretrained features but adds factorized attention. After extracting 1212 patches from AST, we reshape them into a  $101 \times 12$  grid (time  $\times$  frequency). Learnable 2D positional encodings are added. Two dual-attention blocks apply temporal attention (each frequency band attends across time) followed by frequency attention (each time step attends across frequencies). A learnable skip connection, initialized with weight  $-2.0$  (yielding  $\alpha \approx 0.12$ ), blends the attention output with AST’s original CLS token, preserving approximately 88% of pretrained features.

### 4.2.4 M2-Vision: Factorized Space-Time Attention

Video understanding requires both spatial analysis within frames and temporal modeling across frames. Full space-time attention over 25 frames  $\times$  196 patches has prohibitive  $O((25 \times 196)^2) \approx 24$  million attention entries.

Following ViViT’s Model 2 (factorized encoder), we decompose this into spatial attention within each frame ( $O(25 \times 196^2)$ ) followed by temporal attention for each patch position across frames ( $O(196 \times 25^2)$ ), achieving  $22 \times$  speedup. Four factorized attention blocks process ViT’s patch embeddings (shape: batch  $\times$  25  $\times$  196  $\times$  768), with separate learnable spatial and temporal positional encodings. A skip connection preserves ViT’s pretrained features.

## 4.3 M3: CNN Improvements

After M2’s poor results, we investigated whether simple fixes to baseline CNNs could outperform complex attention mechanisms.

### 4.3.1 M3-Audio: Delta MFCCs

The original audio CNN uses 180 features (40 MFCCs, 12 chroma, 128 mel), averaged over time. We hypothesized that adding temporal dynamics without dramatically increasing dimensionality would help. Delta MFCCs capture the first derivative of cepstral coefficients, encoding how

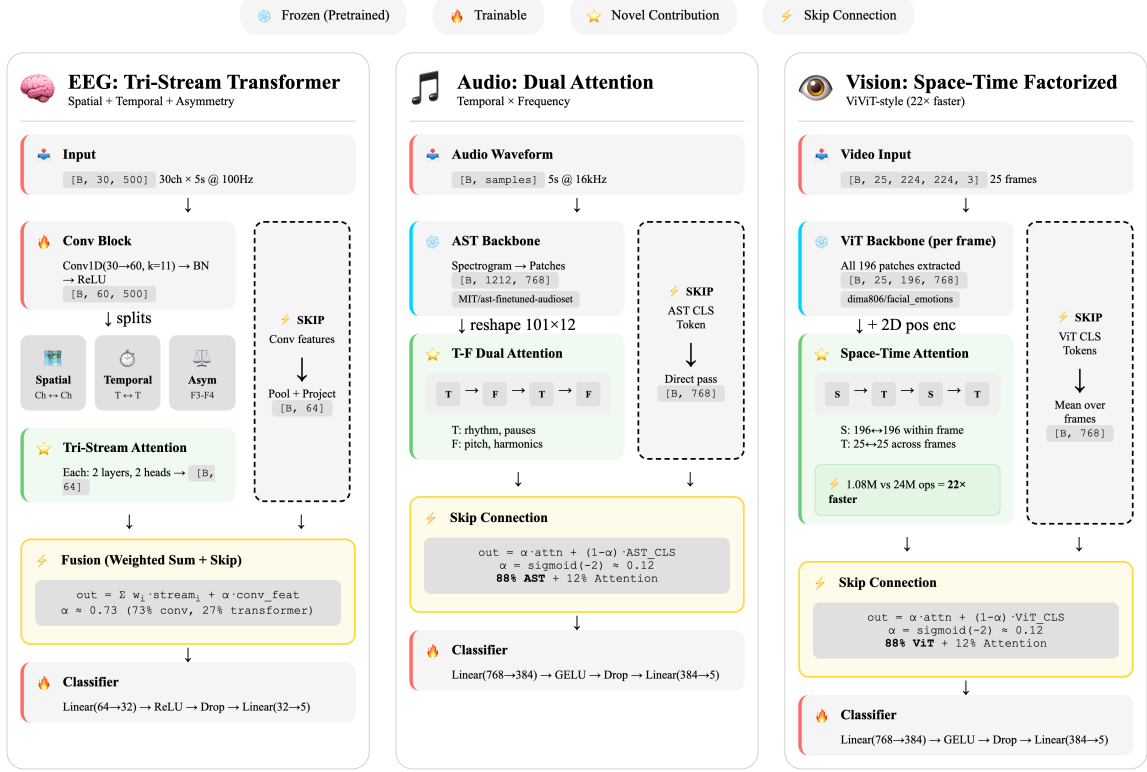


Figure 1: Architecture diagrams for M2: Factorized Attention Mechanisms. Left: EEG Tri-Stream Transformer with spatial, temporal, and asymmetry attention streams. Center: Audio Dual Attention with temporal-frequency factorization over AST features. Right: Vision Space-Time Attention with factorized spatial and temporal attention over ViT embeddings. All architectures include skip connections to preserve pretrained features.

spectral features change over time, which is important for emotional speech where pitch and intensity vary dynamically.

Our modification adds 40 delta MFCC features (also time-averaged), increasing the feature vector from 180 to 220 dimensions. Combined with AdamW optimizer (weight decay 1e-4) and label smoothing (0.1), this minimal change achieved our best audio result.

### 4.3.2 M3-EEG v1: Bug Fixes

We identified a bug in the original EEGNet implementation: `nn.Softmax(dim=1)` in the classifier output, combined with `CrossEntropyLoss` which applies log-softmax internally. This computes  $\log(\text{softmax}(\text{softmax}(x)))$ , damaging gradients. We removed the redundant softmax, added AdamW optimizer with weight decay (0.01), and label smoothing (0.1).

### 4.3.3 M3-EEG v2: Band Power Features

Bug fixes alone proved insufficient because raw time-domain EEG has poor signal-to-noise ratio: approximately 80% of the signal consists of arti-

facts from muscle activity, eye blinks, and electrical noise. Following established practices from SEED dataset research (Zheng and Lu, 2015), we extracted frequency-domain features.

Band power features compute power spectral density using Welch’s method for five frequency bands (delta: 0.5 to 4 Hz, theta: 4 to 8 Hz, alpha: 8 to 13 Hz, beta: 13 to 30 Hz, gamma: 30 to 45 Hz) across all 30 channels, yielding 150 features. Differential entropy features compute  $DE = 0.5 \log(2\pi e \sigma^2)$  for each band-filtered signal, adding another 150 features. Alpha asymmetry features compute  $\ln(P_{\text{right}}^\alpha) - \ln(P_{\text{left}}^\alpha)$  for six hemisphere pairs, adding 6 features that capture frontal asymmetry.

The 306-dimensional feature vector feeds a simple MLP (306 → 128 → 64 → 5) with batch normalization and 50% dropout. Despite having more parameters than EEGNet, this approach operates on meaningful, low-noise features rather than raw high-dimensional signals.

**Concrete Example.** Raw EEG input has 15,000 values ( $30 \text{ channels} \times 500 \text{ time points}$ ) with approximately 20% signal and 80% noise. Band power features compress this to 306 values by: (1) transforming to frequency domain, which averages out temporal noise; (2) focusing on emotion-relevant bands (alpha, beta); and (3) computing asymmetry features grounded in neuroscience. A neural network would need to learn this entire transformation from 280 samples, which is not feasible.

#### 4.3.4 M3-Vision v1: SE Block Fix

We discovered that the original video CNN’s squeeze-excitation block used reduction ratio 1, meaning no dimensionality reduction occurred ( $2048 \rightarrow 2048 \rightarrow 2048$  instead of  $2048 \rightarrow 128 \rightarrow 2048$ ). This defeats the purpose of SE blocks, which learn channel importance through a bottleneck (Hu et al., 2018). We fixed the ratio to 16.

#### 4.3.5 M3-Vision v2: Delta Features

Following our audio success, we added temporal delta features to the video CNN, capturing frame-to-frame changes in facial expression. Delta features compute the difference between consecutive frame representations, encoding expression dynamics that static features miss.

### 5 Experiments and Results

All models were trained on NVIDIA RTX 6000 Ada GPUs (48GB VRAM). We report mean accuracy and standard deviation across all 42 subjects.

Table 1 presents comprehensive results. Three findings emerge clearly.

**M2 Factorized Attention Fails.** All M2 models underperform their respective baselines. The EEG Tri-Stream achieves only 48% (vs. 60% paper baseline), Audio Dual-Attention reaches 49.46% with 7 subjects stuck at random chance (20%), and Vision ViViT-style achieves 69.54% (vs. 74.5% paper baseline). Despite theoretically sound motivation, these complex architectures cannot learn effectively from 280 training samples.

**M3 Simple Fixes Succeed.** Domain-appropriate features improve performance substantially. EEG Band Power achieves 67.62% (+7.62pp over paper), Audio Delta MFCCs achieves 65.56% (+3.66pp), and Vision Delta features achieve 72.68% (+1.28pp over paper CNN). Established signal processing

techniques (frequency analysis, differential features) extract more emotion-relevant information than complex attention mechanisms can learn from limited data. Figure 2 illustrates these architectures.

**Vision: Pretraining Domain Matters.** For Vision, M1’s domain-specific pretraining (75.30%) outperformed all M3 CNN modifications (72.68%), demonstrating that pretraining domain matters more than architectural changes. The ViT model pretrained on facial emotions provides better features than ResNet50 pretrained on ImageNet, even with our improvements.

**Subject Variability.** Table 2 shows substantial individual differences. Subject 17 consistently achieves highest accuracy across all modalities (93.33% vision, 85% audio, 82.5% EEG), suggesting highly expressive emotional displays. Subjects 35 and 12 present persistent challenges, potentially due to subtle expressions or individual physiological differences.

### 6 Analysis: Why M2 Failed

Our M2 architectures failed for three interconnected reasons.

**Destruction of Pretrained Features.** AST and ViT backbones contain valuable features learned from millions of images and audio clips. Our additional attention layers, despite skip connections, modify these representations. The learned skip weight ( $\alpha \approx 0.12$ ) indicates the model tries to preserve pretrained features (88%), but this proves insufficient: the 12% attention contribution still degrades performance.

**Insufficient Training Data.** The EEG Tri-Stream model has 138,401 parameters trained on 280 samples per subject. Standard heuristics suggest parameters should be less than  $10 \times$  training samples for good generalization. Our models exceed this by 5 to  $50 \times$ , leading to overfitting (100% training accuracy but 20 to 80% test accuracy, especially for Audio M2 where 7 subjects achieve exactly 20% random chance).

**Complex Inductive Biases Require Data.** Factorized attention implements sophisticated inductive biases (separate spatial, temporal, and frequency reasoning), but learning to use these biases effectively requires substantial data. On small

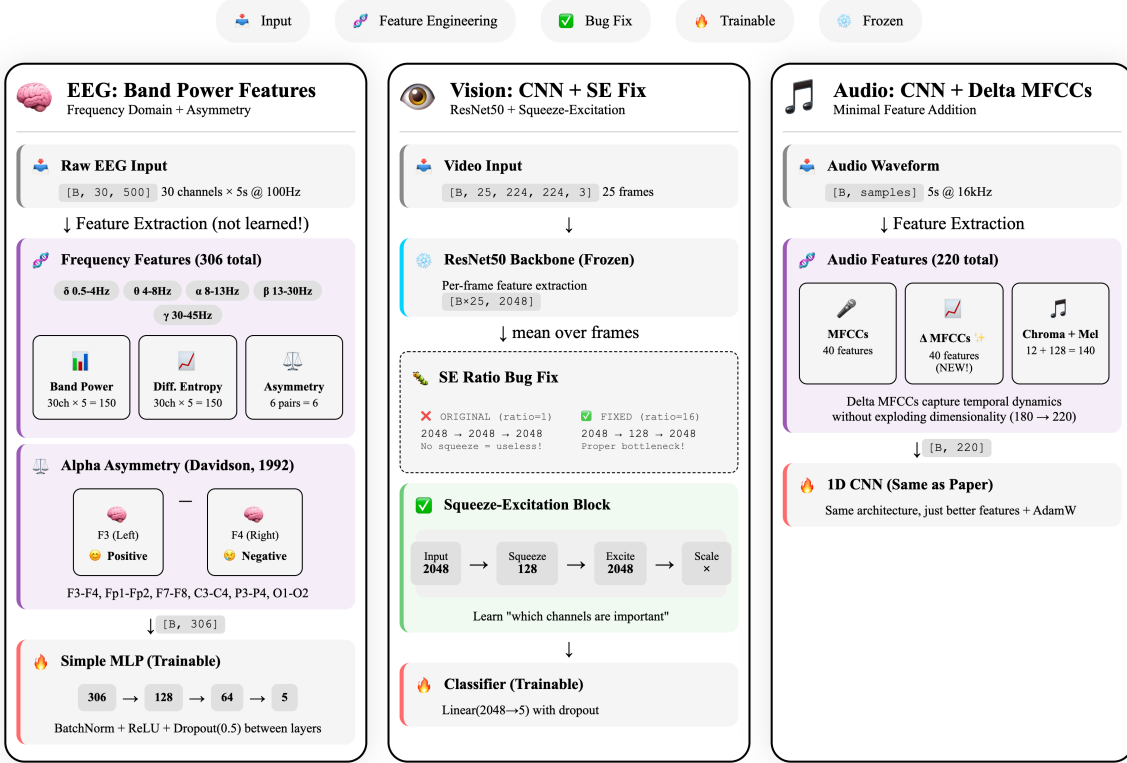


Figure 2: Architecture diagrams for M3: CNN Improvements. Left: EEG Band Power Features with frequency-domain feature extraction (band power, differential entropy, and alpha asymmetry) feeding a simple MLP. Center: Vision CNN with ResNet50 backbone and fixed squeeze-excitation block. Right: Audio CNN with delta MFCC features added to the original feature set.

datasets, the overhead of additional parameters outweighs any architectural benefit.

## 7 Analysis: Why M3 Succeeded

### Domain Knowledge Over Learned Features.

Band power features encode decades of neuroscience research into 306 meaningful dimensions. Alpha asymmetry directly captures Davidson’s frontal asymmetry model. Delta MFCCs encode speech dynamics known to correlate with emotion. These features compress relevant information while discarding noise, something neural networks struggle to learn from limited data.

**Bug Fixes Restore Intended Behavior.** The softmax bug in EEGNet and SE ratio bug in the video CNN were non-obvious implementation errors that degraded baseline performance. Simple fixes recovered significant accuracy without adding complexity.

**Minimal Complexity.** M3 models add minimal parameters over baselines. The 220-feature audio CNN adds only 40 dimensions. The band

power MLP, while larger than EEGNet, operates on preprocessed features rather than raw 15,000-dimensional signals.

## 8 Limitations

Our study has several limitations. First, all experiments use subject-dependent evaluation; cross-subject generalization remains unexplored. Second, the EAV dataset’s conversational paradigm may not generalize to spontaneous emotions. Third, we did not explore multimodal fusion, which may further improve results by combining complementary information across modalities. Fourth, our M2 architectures may benefit from more careful hyperparameter tuning on larger validation sets. Finally, the EAV dataset contains only 42 subjects, limiting statistical power for detecting small effects.

## 9 Conclusion

This study systematically investigated attention mechanisms for multimodal emotion recognition on small datasets. Our findings show that for datasets with approximately 280 training samples

Category	Model	EEG	Audio	Vision
Paper Baselines	CNN	60.00%	61.90%	71.40%
	Transformer	53.50%	62.70%	74.50%
M1: Our Baseline	Transformer	$52.68\% \pm 10.3$	$58.06\% \pm 10.5$	<b>75.30% <math>\pm 10.5</math></b>
M2: Factorized Attn.	EEG Tri-Stream	$48.00\% \pm 12.1$	—	—
	EEGNet-Improved	$58.47\% \pm 11.2$	—	—
	Audio Dual-Attn.	—	$49.46\% \pm 15.8$	—
	Vision ViViT-style	—	—	$69.54\% \pm 12.3$
M3: CNN Improved	EEG v1 (Bug Fix)	$57.66\% \pm 13.7$	—	—
	EEG v2 (Band Power)	<b>67.62% <math>\pm 8.2</math></b>	—	—
	Audio (Delta MFCC)	—	<b>65.56% <math>\pm 9.3</math></b>	—
	Vision v1 (SE Fix)	—	—	$69.42\% \pm 11.9$
	Vision v2 (Delta)	—	—	<b>72.68% <math>\pm 10.8</math></b>

Table 1: Results across all models. **Green** indicates results exceeding paper baselines. M2 factorized attention underperforms across all modalities; M3 simple fixes achieve best results.

Subject	EEG	Audio	Vision
<i>Top Performers</i>			
S17	82.50%	85.00%	93.33%
S6	—	78.33%	94.17%
S20	83.33%	—	91.67%
S24	85.00%	—	—
S2	80.83%	85.00%	—
<i>Difficult Subjects</i>			
S35	46.67%	55.00%	56.67%
S12	—	54.17%	43.33%
S29	56.67%	47.50%	—
S37	—	46.67%	—
S34	54.17%	49.17%	—

Table 2: Subject-level analysis showing best M3 results. S17 is consistently the most expressive subject across all modalities.

per subject, domain-appropriate signal processing outperforms sophisticated neural architectures.

Our best results (EEG 67.62%, +7.62pp; Audio 65.56%, +3.66pp; Vision 75.30%, +0.80pp transformer and 72.68%, +1.28pp CNN) were achieved through simple modifications: frequency-domain features for EEG, delta coefficients for audio and video, and properly pretrained transformers. Meanwhile, our theoretically motivated factorized attention mechanisms (M2) consistently underperformed by 5 to 13 percentage points.

The practical lesson is clear: before adding architectural complexity, researchers should (1) verify baseline implementations for bugs, (2) consider domain-specific feature engineering, and (3) match model capacity to available training data. Future work should evaluate these factorized attention approaches on larger emotion datasets where their sophisticated inductive biases may prove beneficial.

## References

Anurag Arnab, Mostafa Dehghani, Georg Heigold, Chen Sun, Mario Lučić, and Cordelia Schmid. 2021. Vivit: A video vision transformer. In *Proceedings of the IEEE/CVF International Conference on Computer Vision*, pages 6836–6846.

Carlos Busso, Murtaza Bulut, Chi-Chun Lee, Abe Kazemzadeh, Emily Mower, Samuel Kim, Jeanette N Chang, Sungbok Lee, and Shrikanth S Narayanan. 2008. Iemocap: Interactive emotional dyadic motion capture database. In *Language Resources and Evaluation*, volume 42, pages 335–359. Springer.

Richard J Davidson. 1992. Emotion and affective style: Hemispheric substrates. *Psychological Science*, 3(1):39–43.

Yuan Gong, Yu-An Chung, and James Glass. 2021. Ast: Audio spectrogram transformer. *arXiv preprint arXiv:2104.01778*.

Jie Hu, Li Shen, and Gang Sun. 2018. Squeeze-and-excitation networks. In *CVPR*.

Imran Hussain and Sang-Joon Park. 2022. Eegformer: A transformer-based model for eeg signal processing. *IEEE Transactions on Neural Systems and Rehabilitation Engineering*.

Tae-Eui Kim, Byoung-Tak Kim, Jae-Yeon Kim, and Ki-Yong Lee. 2024. Eav: Eeg-audio-video dataset for emotion recognition in conversational contexts. *Scientific Data*, 11:838.

Sander Koelstra, Christian Muhl, Mohammad Soleymani, Jong-Seok Lee, Ashkan Yazdani, Touradj Ebrahimi, Thierry Pun, Anton Nijholt, and Ioannis Patras. 2012. Deap: A database for emotion analysis using physiological signals. *IEEE Transactions on Affective Computing*, 3(1):18–31.

Björn Schuller and 1 others. 2013. The interspeech 2013 computational paralinguistics challenge. *INTERSPEECH*.

Wei-Long Zheng and Bao-Liang Lu. 2015. Investigating critical frequency bands and channels for eeg-based emotion recognition with deep neural networks. *IEEE Transactions on Autonomous Mental Development*.

## A Theoretical Background

This appendix provides comprehensive theoretical foundations for the deep learning models and signal processing techniques used in multimodal emotion recognition, organized by model category (M1, M2, M3).

### A.1 A. Foundations

#### A.1.1 A.1 Emotion Recognition Fundamentals

**Discrete Emotion Theory** proposes that emotions consist of universal basic categories. The EAV dataset uses five discrete classes: Neutral, Anger, Happiness, Sadness, and Calmness. These categories map to Russell's circumplex model of affect along valence (positive/negative) and arousal (high/low) dimensions:

$$\begin{aligned}
 \text{Happiness} &\rightarrow (+\text{valence}, +\text{arousal}) \\
 \text{Anger} &\rightarrow (-\text{valence}, +\text{arousal}) \\
 \text{Sadness} &\rightarrow (-\text{valence}, -\text{arousal}) \\
 \text{Calmness} &\rightarrow (+\text{valence}, -\text{arousal}) \\
 \text{Neutral} &\rightarrow (0, 0)
 \end{aligned} \tag{1}$$

#### A.1.2 A.2 EEG Signal Processing

**Electroencephalography (EEG)** measures electrical activity from neural populations via scalp electrodes. The International 10-20 System specifies electrode placement, where letters indicate brain regions (F=Frontal, C=Central, P=Parietal, O=Occipital, T=Temporal) and numbers indicate hemisphere (odd=left, even=right, z=midline).

The EAV dataset uses 30 channels sampled at 500 Hz. Key electrode pairs for emotion include:

- **F3-F4:** Frontal asymmetry (primary emotion indicator)
- **Fp1-Fp2:** Prefrontal activity
- **C3-C4:** Central sensorimotor

EEG signals are characterized by frequency bands with distinct functional correlates:

Band	Frequency	Function
Delta ( $\delta$ )	0.5–4 Hz	Deep sleep, unconscious processing
Theta ( $\theta$ )	4–8 Hz	Memory encoding, emotional processing
Alpha ( $\alpha$ )	8–13 Hz	Relaxed alertness, frontal asymmetry
Beta ( $\beta$ )	13–30 Hz	Active thinking, concentration
Gamma ( $\gamma$ )	30–45 Hz	High-level cognitive binding

**Davidson's Frontal Asymmetry Model** (1992) establishes that left frontal cortex activation (F3) correlates with approach motivation and positive emotions, while right frontal activation (F4) correlates with withdrawal motivation and negative emotions. The Frontal Asymmetry Index (FAI) quantifies this:

$$\text{FAI} = \ln(P_{F4}^\alpha) - \ln(P_{F3}^\alpha) \tag{2}$$

where  $P^\alpha$  denotes alpha band power. Note that alpha power is inversely related to cortical activity (higher alpha = lower activity), so positive FAI indicates greater left frontal activation (positive valence).

### A.1.3 A.2.1 EEG Preprocessing Pipeline

**Step 1: Downsampling.** Original 500 Hz  $\rightarrow$  100 Hz using polyphase resampling:

$$x_{\text{down}}[n] = \sum_k h[k] \cdot x[Mn - k] \quad (3)$$

where  $M = 5$  is the decimation factor and  $h[k]$  is an anti-aliasing FIR filter.

**Step 2: Bandpass Filtering.** 5th-order Butterworth IIR filter (0.5–45 Hz):

$$|H(j\omega)|^2 = \frac{1}{1 + \left(\frac{\omega}{\omega_c}\right)^{2n}} \quad (4)$$

where  $n = 5$  is the filter order. Transfer function:

$$H(s) = \frac{1}{\prod_{k=1}^n (s - p_k)}, \quad p_k = \omega_c e^{j\pi(2k+n-1)/(2n)} \quad (5)$$

### A.1.4 A.3 Audio Signal Processing

**Mel-Frequency Cepstral Coefficients (MFCCs)** are the standard features for speech analysis, designed to mimic human auditory perception. The extraction pipeline consists of five steps:

**Step 1: Pre-emphasis.** Boost high frequencies to balance the spectrum:

$$y[n] = x[n] - \alpha x[n - 1], \quad \alpha \approx 0.97 \quad (6)$$

**Step 2: Framing and Windowing.** Segment into overlapping frames with Hamming window:

$$x_m[n] = x[n + mH] \cdot w[n], \quad w[n] = 0.54 - 0.46 \cos\left(\frac{2\pi n}{N-1}\right) \quad (7)$$

**Step 3: Short-Time Fourier Transform.**

$$X[k, m] = \sum_{n=0}^{N-1} x_m[n] \cdot e^{-j2\pi kn/N} \quad (8)$$

**Step 4: Mel Filterbank.** Apply triangular filters on mel scale:

$$\text{Mel}(f) = 2595 \log_{10} \left( 1 + \frac{f}{700} \right) \quad (9)$$

**Step 5: Discrete Cosine Transform.** Decorrelate filterbank outputs:

$$c_n = \sum_{m=1}^M \log(S_m) \cos \left[ n \left( m - \frac{1}{2} \right) \frac{\pi}{M} \right] \quad (10)$$

**Delta Features** capture temporal dynamics:

$$\Delta c_t = \frac{\sum_{n=1}^N n(c_{t+n} - c_{t-n})}{2 \sum_{n=1}^N n^2} \quad (11)$$

### A.1.5 A.4 Vision Processing

**Facial Action Coding System (FACS)** (Ekman & Friesen, 1978) decomposes facial expressions into Action Units (AUs)—minimal muscle movements:

Emotion	Typical AUs	Description
Happiness	AU6 + AU12	Cheek raiser + Lip corner puller (Duchenne smile)
Sadness	AU1 + AU4 + AU15	Inner brow raiser + Brow lowerer + Lip corner depressor
Anger	AU4 + AU5 + AU7	Brow lowerer + Upper lid raiser + Lid tightener
Fear	AU1 + AU2 + AU4 + AU20	Brows raised, pulled together, lip stretch
Surprise	AU1 + AU2 + AU5 + AU26	Brow raiser + Upper lid raiser + Jaw drop

### A.1.6 A.5 Transformer Architecture

#### Scaled Dot-Product Attention:

$$\text{Attention}(\mathbf{Q}, \mathbf{K}, \mathbf{V}) = \text{softmax} \left( \frac{\mathbf{Q}\mathbf{K}^T}{\sqrt{d_k}} \right) \mathbf{V} \quad (12)$$

where:

- $\mathbf{Q} = \mathbf{X}\mathbf{W}^Q \in \mathbb{R}^{n \times d_k}$  (queries)
- $\mathbf{K} = \mathbf{X}\mathbf{W}^K \in \mathbb{R}^{n \times d_k}$  (keys)
- $\mathbf{V} = \mathbf{X}\mathbf{W}^V \in \mathbb{R}^{n \times d_v}$  (values)
- $\sqrt{d_k}$  scaling prevents softmax saturation

#### Multi-Head Attention:

$$\text{MHA}(\mathbf{X}) = \text{Concat}(\text{head}_1, \dots, \text{head}_h) \mathbf{W}^O \quad (13)$$

$$\text{head}_i = \text{Attention}(\mathbf{X}\mathbf{W}_i^Q, \mathbf{X}\mathbf{W}_i^K, \mathbf{X}\mathbf{W}_i^V) \quad (14)$$

#### Transformer Encoder Layer:

$$\mathbf{z}'_l = \text{MSA}(\text{LN}(\mathbf{z}_{l-1})) + \mathbf{z}_{l-1} \quad (15)$$

$$\mathbf{z}_l = \text{MLP}(\text{LN}(\mathbf{z}'_l)) + \mathbf{z}'_l \quad (16)$$

Computational complexity is  $O(n^2 \cdot d)$ , quadratic in sequence length  $n$ .

### A.1.7 A.6 CNN Architectures

**EEGNet Architecture.** Uses depthwise separable convolutions for efficient EEG processing:

*Block 1: Temporal Convolution*

$$\mathbf{h}_1 = \text{ELU}(\text{BN}(\text{Conv2D}_{(1, K)}(\mathbf{x}))) \quad (17)$$

where  $K = 300$  at 100Hz captures 3-second temporal patterns.

*Depthwise Convolution:* Learns spatial filters per channel

$$\mathbf{h}_2 = \text{DepthwiseConv}_{(C, 1)}(\mathbf{h}_1) \quad (18)$$

*Block 2: Separable Convolution*

$$\mathbf{h}_3 = \text{SeparableConv}_{(1, 16)}(\mathbf{h}_2) \quad (19)$$

**Parameter Count:** Only  $\sim 2,600$  parameters—ideal for small datasets!

**Squeeze-and-Excitation Blocks.** Learn channel-wise attention:

*Squeeze:* Global average pooling

$$z_c = \frac{1}{H \times W} \sum_{i=1}^H \sum_{j=1}^W x_c(i, j) \quad (20)$$

*Excitation:* Bottleneck MLP with reduction ratio  $r$

$$\mathbf{s} = \sigma(\mathbf{W}_2 \cdot \text{ReLU}(\mathbf{W}_1 \cdot \mathbf{z})) \quad (21)$$

where  $\mathbf{W}_1 \in \mathbb{R}^{C/r \times C}$ ,  $\mathbf{W}_2 \in \mathbb{R}^{C \times C/r}$

*Scale:* Channel reweighting

$$\tilde{\mathbf{x}}_c = s_c \cdot \mathbf{x}_c \quad (22)$$

**Critical Bug in Original Code:**  $r = 1$  means  $\mathbf{W}_1 \in \mathbb{R}^{C \times C}$ —no bottleneck, no squeeze! We fixed to  $r = 16$ .

### A.1.8 A.7 Vision Transformer for Video

#### Patch Embedding:

$$\mathbf{z}_0^i = \mathbf{W}_E \cdot \text{Flatten}(\mathbf{x}_p^i) + \mathbf{e}_{\text{pos}}^i \quad (23)$$

For a  $224 \times 224$  image with  $16 \times 16$  patches:

$$N = \left( \frac{224}{16} \right)^2 = 196 \text{ patches} \quad (24)$$

#### Classification:

$$\hat{y} = \text{MLP}(\text{LN}(\mathbf{z}_L^0)) \quad (25)$$

where  $\mathbf{z}_L^0$  is the [CLS] token output from the final layer.

## A.2 B. Model 1: Baseline Transformers

M1 establishes baseline performance using standard transformer architectures with minimal modifications from pretrained models.

### A.2.1 B.1 M1-EEG: Custom EEG Transformer

Our EEG baseline uses a lightweight custom architecture since no suitable pretrained EEG transformer exists for emotion recognition.

**Convolutional Feature Extraction.** Two 1D convolutions extract local temporal features:

$$\mathbf{h}_1 = \text{ReLU}(\text{BN}(\text{Conv1D}_{30 \rightarrow 30}(\mathbf{x}))), \quad k = 11 \quad (26)$$

$$\mathbf{h}_2 = \text{BN}(\text{Conv1D}_{30 \rightarrow 60}(\mathbf{h}_1)), \quad k = 11 \quad (27)$$

**Transformer Encoding.** Six encoder layers with 4 attention heads process temporal dependencies:

$$\mathbf{z}_l = \text{TransformerBlock}(\mathbf{z}_{l-1}), \quad l \in [1, 6] \quad (28)$$

**Classification.** Mean pooling followed by MLP:

$$\hat{y} = \text{MLP}(\text{MeanPool}(\mathbf{z}_6)) \quad (29)$$

**Limitation:** Standard self-attention treats all time points as a flat sequence, failing to separate spatial (channel) and temporal (time) patterns.

**Result: 52.68%  $\pm$  10.28**

### A.2.2 B.2 M1-Audio: Audio Spectrogram Transformer (AST)

We fine-tune the pretrained AST model (MIT/ast-finetuned-audioset), which treats spectrograms as images using Vision Transformer architecture.

**Patch Embedding.** The spectrogram ( $1024 \times 128$ ) is divided into  $16 \times 16$  patches:

$$N = \left\lfloor \frac{1024 - 16}{10} + 1 \right\rfloor \times \left\lfloor \frac{128 - 16}{10} + 1 \right\rfloor = 101 \times 12 = 1212 \quad (30)$$

#### Two-Stage Training.

1. Stage 1: Freeze backbone, train classifier (LR=5e-4, 10 epochs)
2. Stage 2: Unfreeze all, fine-tune (LR=5e-6, 15 epochs)

**Limitation:** Flattening patches loses the distinction between temporal (rhythm) and frequency (pitch) axes.

**Result: 58.06%  $\pm$  10.54**

### A.2.3 B.3 M1-Vision: Vision Transformer (ViT)

We use a ViT pretrained on facial emotion recognition (dima806/facial\_emotions\_image\_detection).

**Frame-Level Processing.** Each of 25 video frames is processed independently:

$$\hat{y}_{\text{frame}} = \text{ViT}(\mathbf{I}_{\text{frame}}) \quad (31)$$

**Video-Level Prediction.** Frame predictions are averaged:

$$\hat{y}_{\text{video}} = \frac{1}{25} \sum_{f=1}^{25} \hat{y}_f \quad (32)$$

**Limitation:** No temporal modeling across frames—cannot capture facial dynamics.

**Result:** **75.30%  $\pm$  10.45** (exceeds paper baseline by +0.80pp)

## A.3 C. Model 2: Factorized Attention

M2 represents our main architectural contribution: axis-specific factorized attention tailored to each modality's unique structure.

### A.3.1 C.1 Motivation: Why Factorized Attention?

Standard transformers flatten multi-dimensional data into 1D sequences, losing structural information. For emotion recognition:

- **EEG:** Spatial (brain regions) vs temporal (dynamics) vs asymmetry (hemisphere differences)
- **Audio:** Temporal (rhythm) vs frequency (pitch)
- **Video:** Spatial (face regions) vs temporal (expression dynamics)

Factorized attention models these axes separately, providing better inductive bias and computational efficiency.

**Complexity Analysis.** For video with  $T$  frames and  $P$  patches:

$$\text{Full attention: } O((T \cdot P)^2) = O(T^2 P^2) \quad (33)$$

$$\text{Factorized: } O(T \cdot P^2 + P \cdot T^2) \quad (34)$$

For  $T = 25$ ,  $P = 196$ :

$$\text{Speedup} = \frac{(25 \times 196)^2}{25 \times 196^2 + 196 \times 25^2} = \frac{24,010,000}{1,082,900} \approx 22 \times \quad (35)$$

### A.3.2 C.2 M2-EEG v1: Tri-Stream Spatial-Temporal-Asymmetry Transformer

**Novel Contribution:** We introduce a third attention stream for hemispheric asymmetry, based on Davidson's frontal asymmetry model.

**Architecture.** Input EEG (30 channels, 500 samples) passes through convolutional feature extraction, then branches into three parallel attention streams:

**Spatial Stream.** Channels attend to channels at each time point:

$$\mathbf{h}_{\text{spatial}} = \text{Attn}(\mathbf{z}^{(t)}), \quad \mathbf{z}^{(t)} \in \mathbb{R}^{C \times d} \quad (36)$$

This captures which brain regions interact (functional connectivity).

**Temporal Stream.** Time points attend to time points for each channel:

$$\mathbf{h}_{\text{temporal}} = \text{Attn}(\mathbf{z}^{(c)}), \quad \mathbf{z}^{(c)} \in \mathbb{R}^{T \times d} \quad (37)$$

This captures event-related dynamics.

**Asymmetry Stream.** We compute difference signals for six hemisphere pairs:

$$\mathbf{a}_{\text{asym}}(t) = \begin{bmatrix} x_{F3}(t) - x_{F4}(t) & (\text{frontal, } 1.2 \times \text{ boost}) \\ x_{Fp1}(t) - x_{Fp2}(t) & (\text{prefrontal}) \\ x_{F7}(t) - x_{F8}(t) & (\text{lateral frontal}) \\ x_{C3}(t) - x_{C4}(t) & (\text{central}) \\ x_{P3}(t) - x_{P4}(t) & (\text{parietal}) \\ x_{O1}(t) - x_{O2}(t) & (\text{occipital}) \end{bmatrix} \quad (38)$$

The F3-F4 pair receives a subtle  $1.2 \times$  attention weight boost based on its established importance for emotional valence.

**Fusion.** Streams are combined via learned softmax weights:

$$\mathbf{h}_{\text{fused}} = \sum_{i \in \{\text{s,t,a}\}} w_i \cdot \mathbf{h}_i, \quad w_i = \text{softmax}(\mathbf{W}_{\text{gate}}[\mathbf{h}_s; \mathbf{h}_t; \mathbf{h}_a]) \quad (39)$$

**Skip Connection.** A learnable skip preserves convolutional features:

$$\mathbf{h}_{\text{out}} = \alpha \cdot \mathbf{h}_{\text{fused}} + (1 - \alpha) \cdot \mathbf{h}_{\text{conv}} \quad (40)$$

where  $\alpha = \sigma(w)$  with  $w$  initialized to yield  $\alpha \approx 0.27$ .

**Model Variants:**

Size	Params	Layers	Heads
Small (recommended)	138,401	2	2
Base	419,201	3	4
Large	1,626,305	4	8

**Result:**  $\sim 48\%$  (fails—too complex for 280 samples)

**Failure Analysis:** With 138K parameters and 280 training samples, the model has  $50 \times$  more parameters than data points, leading to severe overfitting. The sophisticated tri-stream architecture cannot learn meaningful patterns from such limited data.

### A.3.3 C.3 M2-EEG v2: EEGNet-Improved

As a literature-based alternative, we enhanced EEGNet with proven techniques:

**Squeeze-Excitation Blocks.** Learn channel importance:

$$\mathbf{s} = \sigma(\mathbf{W}_2 \cdot \text{ReLU}(\mathbf{W}_1 \cdot \text{GAP}(\mathbf{x}))) \quad (41)$$

$$\tilde{\mathbf{x}}_c = s_c \cdot \mathbf{x}_c \quad (42)$$

**Multi-Scale Temporal Convolution.** Parallel convolutions with kernels [16, 32, 64] capture different temporal scales.

**Residual Connections.** Help gradient flow in deeper networks.

**Additional Improvements:** Label smoothing (0.1), AdamW with weight decay (1e-3), cosine annealing LR, data augmentation (amplitude scaling, Gaussian noise, time shift).

**Result:**  $58.47\% \pm 12.56$  (approaches paper baseline)

### A.3.4 C.4 M2-Audio: Temporal-Frequency Dual Attention

**Core Idea.** Preserve AST’s pretrained features while adding axis-specific attention.

**Grid Reconstruction.** Reshape AST’s 1212 patch embeddings into a  $101 \times 12$  grid (time  $\times$  frequency):

$$\mathbf{Z} \in \mathbb{R}^{B \times 1212 \times 768} \rightarrow \mathbf{Z} \in \mathbb{R}^{B \times 101 \times 12 \times 768} \quad (43)$$

**2D Positional Encoding.** Add learnable temporal and frequency position embeddings:

$$\tilde{\mathbf{Z}} = \mathbf{Z} + \mathbf{E}_{\text{temporal}} + \mathbf{E}_{\text{freq}} \quad (44)$$

**Dual Attention Blocks.** Two blocks apply sequential attention:

*Temporal Attention:* Each frequency band attends across time:

$$\mathbf{h}_{\text{temp}}^{(f)} = \text{Attn}(\tilde{\mathbf{Z}}[:, :, f, :]), \quad f \in [1, 12] \quad (45)$$

*Frequency Attention:* Each time step attends across frequency:

$$\mathbf{h}_{\text{freq}}^{(t)} = \text{Attn}(\mathbf{h}_{\text{temp}}[:, t, :, :]), \quad t \in [1, 101] \quad (46)$$

**Skip Connection.** Critical for preserving AST features:

$$\mathbf{h}_{\text{out}} = \alpha \cdot \text{Pool}(\mathbf{h}_{\text{freq}}) + (1 - \alpha) \cdot \mathbf{z}_{\text{CLS}} \quad (47)$$

where  $\alpha = \sigma(-2.0) \approx 0.12$  initially (88% AST, 12% attention).

**Result: 49.46%** (fails—7 subjects stuck at 20% random chance)

**Failure Analysis:** Despite preserving 88% of AST features, the additional attention layers introduce noise that corrupts the pretrained representations. On small data, even minor corruption cannot be recovered.

### A.3.5 C.5 M2-Vision: Factorized Space-Time Attention

**Architecture.** Following ViViT Model 2 (factorized encoder), we apply:

**Spatial Attention.** Within each frame, patches attend to patches:

$$\mathbf{h}_{\text{spatial}}^{(t)} = \text{Attn}(\mathbf{z}^{(t)}), \quad t \in [1, 25] \quad (48)$$

**Temporal Attention.** For each patch position, frames attend to frames:

$$\mathbf{h}_{\text{temporal}}^{(p)} = \text{Attn}(\mathbf{h}_{\text{spatial}}^{(p)}), \quad p \in [1, 196] \quad (49)$$

**Skip Connection.** Preserves ViT features with learnable  $\alpha$ .

**Result: 69.54%** (best M2 result, but still -5pp below baseline)

**Partial Success Analysis:** Skip connection helps preserve pretrained features. However, the additional spatial-temporal attention layers still degrade performance compared to simple frame averaging, suggesting that temporal modeling is unnecessary for this dataset’s short video clips.

## A.4 D. Model 3: CNN Improvements

After M2’s failures, we investigated whether simple fixes to baseline CNNs could outperform complex attention mechanisms.

### A.4.1 D.1 Philosophy: Simple Fixes Over Complex Architectures

M2’s failures revealed that:

1. Complex models overfit on small datasets
2. Pretrained features are destroyed by additional layers
3. The baseline authors likely tried complex approaches first

M3 philosophy: Fix bugs, add minimal domain-appropriate features, preserve working architecture.

### A.4.2 D.2 M3-Audio: Delta MFCCs

**Bug Fix:** Replace Adam with AdamW (proper weight decay).

**Minimal Addition:** Add 40 delta MFCC features ( $180 \rightarrow 220$  total):

$$\mathbf{x} = [\underbrace{\text{MFCC}_{1:40}}_{\text{original}}, \underbrace{\Delta \text{MFCC}_{1:40}}_{\text{added}}, \text{Chroma}_{1:12}, \text{Mel}_{1:128}] \quad (50)$$

**Why Not Temporal Features?** Keeping full temporal MFCCs ( $40 \times 100 = 4000$  values) would cause massive overfitting with 280 samples. Time-averaged delta features capture dynamics without dimensional explosion.

**Training:** AdamW (weight decay 1e-4), label smoothing (0.1).

**Result: 65.56%  $\pm$  9.30** (+3.66pp over paper baseline)

### A.4.3 D.3 M3-EEG v1: Bug Fixes Only

**Critical Bug Found:** The original EEGNet classifier contained `nn.Softmax(dim=1)` before the loss function. Combined with `CrossEntropyLoss` (which applies log-softmax internally), this computes:

$$\mathcal{L}_{\text{wrong}} = -\log(\text{softmax}(\text{softmax}(\mathbf{z}))) \quad (51)$$

This double softmax severely damages gradients—the outer softmax on already-normalized probabilities produces near-uniform distributions, destroying learning signal.

**Fix:** Remove `nn.Softmax` from classifier, use raw logits with `CrossEntropyLoss`.

**Additional Changes:** AdamW (weight decay 0.01), label smoothing (0.1).

**Result: 57.66%  $\pm$  13.66** (-2.34pp below paper baseline)

**Analysis:** Bug fix alone insufficient. Raw time-domain EEG has poor signal-to-noise ratio ( $\sim 80\%$  artifacts from muscle, eye, and electrical noise).

### A.4.4 D.4 M3-EEG v2: Band Power Features (Best EEG Result)

**Key Insight:** Instead of learning frequency decomposition from raw EEG (15,000 values), extract established frequency-domain features first.

**Feature Extraction Pipeline:**

**1. Band Power (150 features).** For each channel  $c$  and frequency band  $b$ , compute power spectral density using Welch's method:

$$P_{c,b} = \int_{f_{\text{low}}^b}^{f_{\text{high}}^b} P_{xx}^{(c)}(f) df \quad (52)$$

where  $P_{xx}(f)$  is estimated via:

$$P_{xx}(f) = \frac{1}{KL} \sum_{k=0}^{K-1} \left| \sum_{n=0}^{L-1} x_k[n] w[n] e^{-j2\pi f n/L} \right|^2 \quad (53)$$

Features: 30 channels  $\times$  5 bands = 150.

**2. Differential Entropy (150 features).** For each band-filtered signal assumed Gaussian:

$$\text{DE}_{c,b} = \frac{1}{2} \log(2\pi e \sigma_{c,b}^2) \quad (54)$$

This is standard in SEED dataset literature. Features:  $30 \times 5 = 150$ .

**3. Alpha Asymmetry (6 features).** Following Davidson's model:

$$\text{Asym}_{ij} = \ln(P_{\alpha,j}) - \ln(P_{\alpha,i}) \quad (55)$$

for pairs (F3,F4), (Fp1,Fp2), (F7,F8), (C3,C4), (P3,P4), (O1,O2).

**Total: 306 features.**

**Classifier:** Simple MLP:

$$306 \xrightarrow{\text{Linear}} 128 \xrightarrow{\text{BN,ReLU,Drop}} 64 \xrightarrow{\text{BN,ReLU,Drop}} 5 \quad (56)$$

**Why This Works:**

Aspect	Raw EEG (v1)	Band Power (v2)
Input dimension	15,000	306
Signal-to-noise	$\sim 20\%$	High (averaged)
Frequency info	Must learn	Pre-extracted
Asymmetry info	Not explicit	6 dedicated features

**Result: 67.62%  $\pm$  7.89** (+7.62pp over paper baseline)

#### A.4.5 D.5 M3-Vision v1: SE Block Fix

**Bug Found:** The original squeeze-excitation block used reduction ratio  $r = 1$ :

$$\mathbf{W}_1 \in \mathbb{R}^{C \times C}, \quad \mathbf{W}_2 \in \mathbb{R}^{C \times C} \quad (57)$$

With  $r = 1$ , there is no bottleneck—the “squeeze” does not squeeze! The SE block degenerates to a pointless transformation.

**Fix:** Set  $r = 16$  for proper bottleneck:

$$\mathbf{W}_1 \in \mathbb{R}^{(C/16) \times C}, \quad \mathbf{W}_2 \in \mathbb{R}^{C \times (C/16)} \quad (58)$$

For  $C = 2048$ :  $2048 \rightarrow 128 \rightarrow 2048$  (proper squeeze-excitation).

**Result:** **69.42%  $\pm$  10.81** (-1.98pp vs paper baseline)

#### A.4.6 D.6 M3-Vision v2: Delta Features (Best CNN)

Following audio success, we add frame-to-frame delta features capturing expression dynamics. The delta features compute the difference between consecutive frame representations:

$$\mathbf{d}_t = \mathbf{f}_{t+1} - \mathbf{f}_t \quad (59)$$

where  $\mathbf{f}_t$  is the frame feature vector from the backbone.

The final representation combines averaged static and delta features:

$$\mathbf{x} = \left[ \frac{1}{T} \sum_{t=1}^T \mathbf{f}_t, \frac{1}{T-1} \sum_{t=1}^{T-1} \mathbf{d}_t \right] \quad (60)$$

**Result:** **72.68%  $\pm$  9.56** (+1.28pp over paper CNN baseline)

### A.5 E. Optimization and Regularization

#### A.5.1 E.1 Loss Functions

**Cross-Entropy Loss:**

$$\mathcal{L}_{\text{CE}} = - \sum_{c=1}^C y_c \log(\hat{y}_c) \quad (61)$$

**Label Smoothing.** Softens targets to prevent overconfidence:

$$y'_c = (1 - \epsilon)y_c + \frac{\epsilon}{C} \quad (62)$$

With  $\epsilon = 0.1$  and  $C = 5$ :  $[0, 0, 1, 0, 0] \rightarrow [0.02, 0.02, 0.92, 0.02, 0.02]$

#### A.5.2 E.2 AdamW Optimizer

$$\theta_t = \theta_{t-1} - \alpha \left( \frac{\hat{m}_t}{\sqrt{\hat{v}_t} + \epsilon} + \lambda \theta_{t-1} \right) \quad (63)$$

Key difference from Adam: weight decay  $\lambda\theta$  is applied directly, not scaled by adaptive learning rate.

#### A.5.3 E.3 Regularization

**Dropout:** Randomly zeros elements with probability  $p$ :

$$\tilde{h}_i = \frac{h_i}{1-p} \cdot \mathbb{1}[\text{Bernoulli}(1-p)] \quad (64)$$

**Batch Normalization:**

$$\hat{x}_i = \gamma \frac{x_i - \mu_B}{\sqrt{\sigma_B^2 + \epsilon}} + \beta \quad (65)$$

**Gradient Clipping:** Prevents exploding gradients:

$$\mathbf{g}' = \min \left( 1, \frac{\tau}{\|\mathbf{g}\|} \right) \mathbf{g}, \quad \tau = 1.0 \quad (66)$$

#### A.5.4 E.4 Skip Connections in M2

Critical for preserving pretrained features:

$$\mathbf{h}_{\text{out}} = \alpha \cdot \mathbf{h}_{\text{new}} + (1 - \alpha) \cdot \mathbf{h}_{\text{pretrained}} \quad (67)$$

**Initialization:**  $\alpha = \sigma(w)$  with  $w = -2.0$  yields  $\alpha \approx 0.12$  (88% pretrained, 12% new).

**Observation:** After training,  $\alpha$  remains near 0.12—the model learns that pretrained features dominate on small data.

#### A.6 F. Model Complexity Analysis

Model	Params	Trainable	Result
<i>EEG Models</i>			
EEGNet (Paper)	2,600	2,600	60.0%
M3-EEG v1 (Bug Fix)	2,600	2,600	57.66%
M3-EEG v2 (Band Power)	~48K	~48K	<b>67.62%</b>
M2-EEGNet-Improved	36,501	36,501	58.47%
M2-Tri-Stream (small)	138,401	138,401	~48%
<i>Audio Models</i>			
AST (M1)	87M	~4K	58.06%
M3-Audio (Delta)	87M	~5K	<b>65.56%</b>
M2-Dual Attention	87M	~12M	49.46%
<i>Vision Models</i>			
ViT (M1)	86M	~4K	<b>75.30%</b>
M3-Vision v1 (SE Fix)	23M	23M	69.42%
M3-Vision v2 (Delta)	23M	23M	<b>72.68%</b>
M2-Factorized	86M	~12M	69.54%

**Rule of Thumb:** Trainable parameters should be  $<10\times$  training samples. With 280 samples, this suggests  $<2,800$  parameters for optimal generalization.

**Observation:** M3-EEG v2 succeeds despite 48K parameters because it operates on meaningful 306-dimensional features rather than noisy 15,000-dimensional raw signals.

#### A.7 G. Data Augmentation

##### EEG:

- Amplitude scaling:  $\tilde{x} = \alpha x$ ,  $\alpha \sim \mathcal{U}(0.9, 1.1)$
- Gaussian noise:  $\tilde{x} = x + \epsilon$ ,  $\epsilon \sim \mathcal{N}(0, 0.01)$
- Time shift: Circular shift by  $\pm 10\%$

##### Audio (SpecAugment):

- Time masking: Zero  $t$  consecutive frames,  $t \sim \mathcal{U}(0, T_{\text{max}})$
- Frequency masking: Zero  $f$  consecutive bins,  $f \sim \mathcal{U}(0, F_{\text{max}})$

##### Video:

- Horizontal flip with  $p = 0.5$
- Color jitter (brightness, contrast, saturation)
- Random erasing (simulates occlusion)

## A.8 H. Evaluation Metrics

### A.8.1 H.1 Accuracy

$$\text{Accuracy} = \frac{\text{TP} + \text{TN}}{\text{TP} + \text{TN} + \text{FP} + \text{FN}} = \frac{\text{Correct Predictions}}{\text{Total Predictions}} \quad (68)$$

### A.8.2 H.2 F1 Score (Weighted)

Per-class metrics:

$$\text{Precision}_c = \frac{\text{TP}_c}{\text{TP}_c + \text{FP}_c}, \quad \text{Recall}_c = \frac{\text{TP}_c}{\text{TP}_c + \text{FN}_c} \quad (69)$$

F1 Score:

$$\text{F1}_c = \frac{2 \cdot \text{Precision}_c \cdot \text{Recall}_c}{\text{Precision}_c + \text{Recall}_c} \quad (70)$$

Weighted Average:

$$\text{F1}_{\text{weighted}} = \sum_{c=1}^C \frac{n_c}{N} \cdot \text{F1}_c \quad (71)$$

where  $n_c$  is the number of samples in class  $c$ .

## A.9 I. Analysis: Why Methods Failed or Succeeded

### A.9.1 I.1 Why M2 Factorized Attention Failed

1. **Destruction of Pretrained Features:** AST and ViT backbones contain valuable features learned from millions of samples. Our attention layers, despite skip connections ( $\alpha \approx 0.12$ ), still corrupt these representations.
2. **Insufficient Training Data:** With 280 samples and 138K+ parameters, M2 models have  $50\times$  more parameters than data points. Standard heuristics suggest  $<10\times$  for good generalization.
3. **Complex Inductive Biases Require Data:** Factorized attention implements sophisticated biases (separate spatial/temporal reasoning), but learning to use them requires substantial data.

**Evidence:** M2 Audio had 7/42 subjects stuck at exactly 20% (random chance for 5 classes), indicating complete failure to learn.

### A.9.2 I.2 Why M3 Simple Fixes Succeeded

1. **Domain Knowledge Over Learned Features:** Band power features encode decades of neuroscience research into 306 meaningful dimensions. Delta MFCCs encode known speech dynamics.
2. **Bug Fixes Restore Intended Behavior:** The softmax bug and SE ratio bug were non-obvious errors degrading baseline performance.
3. **Minimal Complexity:** M3 adds minimal parameters. The 220-feature audio CNN adds only 40 dimensions over baseline.

**Key Insight:** With  $\sim 280$  training samples, **fixing bugs** is more valuable than **adding features**.